

SUPPLEMENTAL MATERIALS

Ketone Ester Treatment Improves Cardiac Function and Reduces Pathologic Remodeling in Pre-clinical Models of Heart Failure

Salva R. Yurista MD PhD*¹, Timothy R. Matsuura PhD*², Herman H.W. Silljé PhD¹, Kirsten T. Nijholt BS¹, Kendra S McDaid BS², Swapnil V. Shewale PhD², Teresa C. Leone BS², John C. Newman MD PhD³, Eric Verdin MD³, Dirk J. van Veldhuisen MD PhD¹, Rudolf A. de Boer MD PhD¹, Daniel P. Kelly MD^{2#}, B. Daan Westenbrink MD PhD^{1#}

From the

1. Department of Cardiology, University Medical Center Groningen, University of Groningen, Groningen, The Netherlands
2. Cardiovascular Institute, Department of Medicine, Perelman School of Medicine at the University of Pennsylvania, Philadelphia, PA 19104, USA
3. Buck Institute for Research on Aging; Division of Geriatrics, University of California, San Francisco, USA

Corresponding author:

B. Daan Westenbrink MD PhD

Department of Cardiology

University Medical Center Groningen

PO Box 30.001, Groningen 9700 RB,

The Netherlands

Phone: +31 50 361 2355 / Fax: +31 50 361 4391 / E-mail: b.d.westenbrink@umcg.nl

SUPPLEMENTAL METHODS

KE-1 ester formulations

To establish an effective oral ketone supplementation in mice we used a ketone diester consisting of a central β HB flanked by two six carbon chains (A hexanoyl-hexyl-(R)-3-hydroxybutyrate (AK Scientific, Union City, CA, US), KE-1, Figure 1A). This ester is hydrolysed following ingestion to yield one molecule of β HB and two medium-chain C6 fatty acid moieties that also provide substrate for ketogenesis. We formulated diets containing 10% or 15% w/w KE-1 to closely match the macronutrient profile of the control diet (Chow) (Table 1).

Animal studies

Mouse studies

Four weeks after initial sham or MI surgery, mice failing to meet echocardiographic criteria for sufficient TAC gradient and infarct size were excluded by a researcher (SVS) blinded to treatment. TAC/MI surgery was performed on 53 mice (26 in Chow group, 27 in KE-1 group). A total of 8 mice were excluded due to low TAC gradient or small MI (6 in Chow group, 2 in KE-1 group).

Rat studies

Six weeks after surgery, rats were anesthetized, blood was drawn and the hearts were rapidly excised for further analysis. Rats with an infarct size of less than 15% were excluded from analysis as these small infarcts are hemodynamically fully compensated. MI surgery was performed on 77 rats. Ten rats (13%) died during the surgical procedure, all remaining rats survived the rest of the study. A total of 6 rats with an infarct < 15 % of the LV were excluded from further analysis (4 rats in early group and 2 rats in late group), leaving a total of 61 rats for the analysis. The experimental protocol is illustrated in Figure 3A.

Echocardiography

Four weeks after surgery, ultrasound examination was performed on mice using a Fujifilm VisualSonics Ultrasound System (Visualsonics Inc, Toronto, ON, Canada). Long-axis 2D and Doppler ultrasound examination of the TAC gradient were obtained as previously described.^{27,15} Two weeks after surgery and 1 week before termination, the M-mode and 2D echocardiography was performed on rats using a Vivid 7 echo machine (GE Healthcare) equipped with a 10-MHz phase array linear transducer for serially assessment of cardiac structure and function as previously described.³ The echo studies were performed by a blinded investigator (BDW) and measurements were validated by external observer.

Invasive hemodynamic measurements

Prior to sacrifice, invasive hemodynamics were analysed by aortic and LV catheterization as previously described.²⁸ The right carotid artery was isolated, punctured, and a 1.9 F rat pressure-volume catheter (Scisense, London, Ontario, Canada) was inserted into the right carotid artery. The tip of the catheter was advanced through the aorta into the LV cavity. Heart rate (HR), aortic systolic and diastolic blood pressure (SBP and DBP) and maximal rates of increase and decrease in developed LV pressure (dp/dt_{max} and dp/dt_{min}) were determined. The data were acquired using a PowerLab data acquisition system (ADInstruments, Colorado Springs, CO) and analysed with LabChart 8 software.

Infarct size, cardiomyocyte size and interstitial fibrosis measurement

Rats were euthanized under isoflurane anaesthesia. Heart were rapidly excised and weighed. The mid-papillary slice of the LV was fixed in 4% formaldehyde and embedded in paraffin. Masson's trichrome staining was also used to evaluate infarct size and the extent of interstitial fibrosis in the non-infarcted LV, as described previously.²⁸⁻²⁹ The whole tissue section was scanned with Hamamatsu scanner and quantified using Aperio ImageScope software. FITC labelled wheat germ agglutinin

(WGA) was used to determine cardiomyocyte size as previously described.²⁸ Cardiomyocyte cross-sectional area were measured using image analysis (Zeiss KS400, Germany) and quantified using ImageJ software (National Institutes of Health, Bethesda, MD, USA). The investigators analysing the data were blinded to the treatment allocation.

Blood and plasma measurements

Blood was obtained from mice via needle prick of the tail followed by immediate measurement of β HB concentration with a Precision Xtra blood ketone meter (Abbott, Columbus, OH). To characterize ketonemia induced by KE-1 diet, β HB measurements were taken during the day (09:00 – 13:00) and at night (00:00 – 02:00). To assess ketonemia in rats, 0.5 ml of blood was drawn from the tail vein during fasting (09:00-10:30) and feeding hours (22:00-22:30), and anti-coagulated with perchloric acid (PCA). At sacrifice, 8 ml of blood was drawn from the abdominal aorta and either anti-coagulated with heparin or EDTA. Plasma creatinine, sodium and potassium were measured by the Roche/Hitachi Cobas system (Roche, Germany). Plasma beta-hydroxybutyrate concentrations were quantified using Autokit 3-HB (Wako Chemicals, Germany). Circulating hormones were measured by a rat ultrasensitive insulin ELISA kit (80-INSRT-E01, ALPCO) and Glucagon ELISA (48-GLUHU-E01, ALPCO) according to the manufacturer's instructions.

Quantitative real-time PCR

RNA was isolated from the non-infarcted LV using TRIzol reagent (Invitrogen Corp., CA, USA) and quantified by the NanoDrop device as previously described.^{28,30} mRNA levels obtained by a quantitative real-time polymerase chain reaction (RT-PCR) using CFX384 Touch Real-Time PCR Detection System (Bio-Rad Laboratories, Veenendaal, The Netherlands). 36B4 reference gene was used to correct all measured mRNA expression. Primer sequences can be found in the Supplementary Table I.

Mitochondrial DNA (mtDNA)-to-nuclear DNA (nDNA) ratio and mtDNA damage

Total DNA including mtDNA was extracted from the non-infarcted left ventricle using Nucleospin® Tissue XS (Macherey-Nagel GmbH&Co. KG, Düren, Germany). mtDNA-to-nDNA ratio was determined by qRT-PCR, as described previously.²⁸ Expression of mitochondrial genes were corrected for nuclear gene expressions values, and the calculated values were expressed relative to the control group per experiment. Relative levels of damage in mtDNA was measured by using semi-long real time-PCR amplification of mtDNA fragments of different lengths, as described before.³ Primer sequences are listed in Table I of the Data Supplement.

Western blot

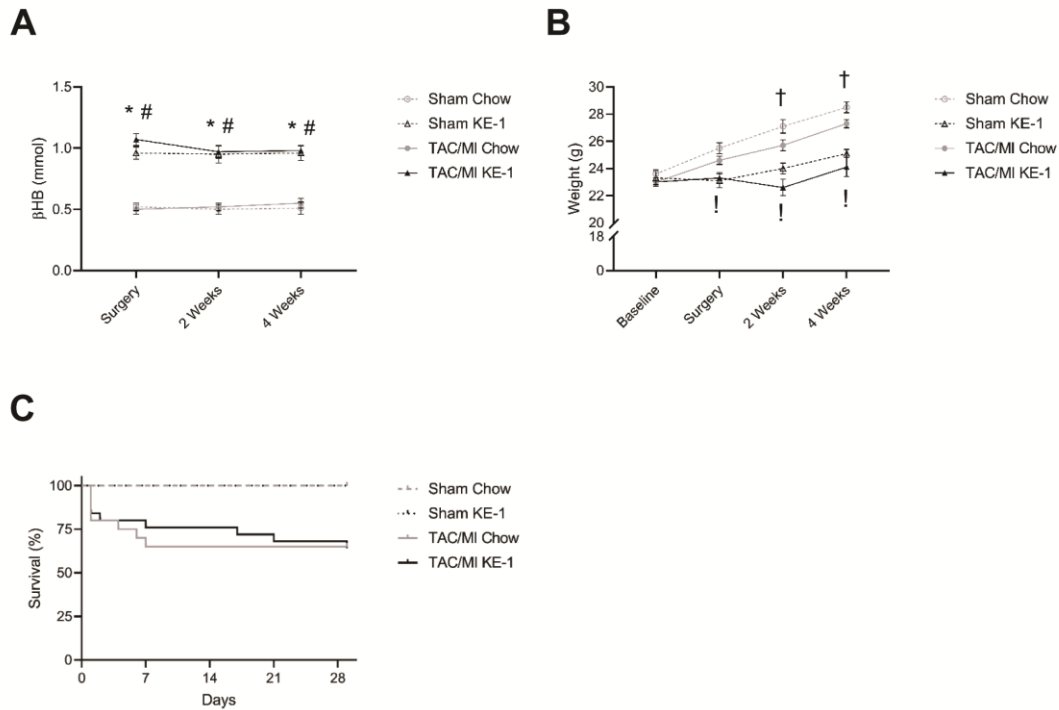
Frozen LV tissue was homogenized and quantified as described before.²⁸ Immunoblotting was performed using primary antibodies from the following commercial suppliers: OXCT1 / SCOT (#ab105320; Abcam, Cambridge, UK), GAPDH (#10R-G109A; Fitzgerald Industries International, Acton, MA, USA). Immunoblots were incubated with appropriate secondary antibodies for 1 hour at room temperature. Signals were detected by ECL (ParkinElmer, Waltham, MA, USA). Blots were quantified using ImageJ software (NIH, Bethesda, MD, USA). The density of each band was normalized to GAPDH acting as a loading control and presented as fold change over Sham-Chow group.

ATP measurements

ATP concentrations in the LV were measured using an ATP Assay Kit (colorimetric/fluorometric) from Abcam (#ab83355, Cambridge, UK) according to the manufacturer's instructions. Results were normalized by protein concentrations of each test, as previously described.²⁸

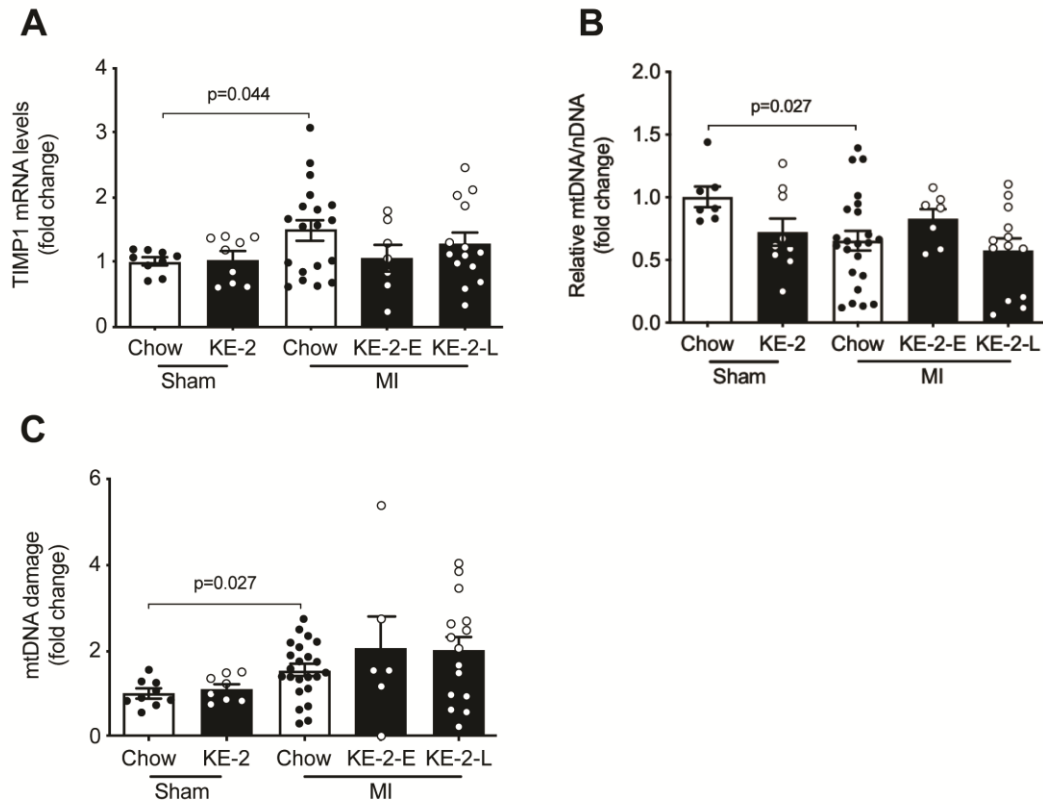
SUPPLEMENTAL FIGURES

Supplemental Figure I



Supplemental Figure I. Effect of ketone ester diet on ketonemia, body weight, and survival in a mouse model of heart failure. (A) Levels of blood β -hydroxybutyrate (BHB) at night in mice fed C6x2-BHB ketone ester (KE-1) or Chow diet. N=11-25, * p <0.05 Sham Chow vs. Sham KE-1, # p <0.05 TAC/MI Chow vs. TAC/MI KE-1, 2-way ANOVA with Tukey multiple comparison test. Data are presented as means \pm SEM. **(B)** Body weight of mice throughout duration of heart failure protocol. N=11-25, * p <0.05 Sham Chow vs. Sham KE-1, † p <0.05 Sham Chow vs. TAC/MI Chow, 2-way ANOVA with Tukey multiple comparison test. **(C)** Survival curve of each surgery and diet group (n=11-25).

Supplemental Figure II



Supplemental Figure II. Effects of ketone ester supplementation on markers of cardiac fibrosis, mitochondrial DNA content and mitochondrial DNA damage in a rat model of heart failure. (A) Levels of mRNA encoding tissue inhibitor of metalloproteinases 1 (TIMP-1) normalized to 36b4 shown as arbitrary units (AU) normalized to the value of Sham Chow-control (+1.0) (n=7-22). **(B)**, Mitochondrial DNA (mtDNA) to nuclear DNA (nDNA) ratio normalized to the value of Sham Chow-control (n=7-22) **(C)** Semi long run PCR of specific mtDNA fragments were used to determine oxidative damage to mtDNA (n=7-22). KE-2-E, KE-2-early; KE-2-L, KE-2-late. Kruskal–Wallis test with Dunn's multiple comparisons test.

SUPPLEMENTAL TABLES I-II

Supplemental Table I. List of primers for qRT-PCR

Gene	Forward primer sequence	Reverse primer sequence
ANP	ATGGGCTCCTTCTCCATCAC	TCTACCGGCATCTTCTCCTC
COL1A1	ACAGCGTAGCCTACATGG	AAGTTCCGGTGTGACTCG
TIMP1	AGAGCCTCTGTGGATATGTC	CTCAGATTATGCCAGGGAAC
MCT1	GGCACCTCTTCTGGAATGCT	GCCCCTCAAACCCACACATA
Bdh1	TCCTGAGAAGGGAATGTGGG	AGTGAACTCCACCTCCCCAA
36B4	GTTGCCTCAGTGCCTCACTC	GCAGCCGCAAATGCAGATGG
TRPM-2 short fragment	GTACAACGAGCTGCTTCATTCC	GCACCTCTAAGAGGCATCCATC
CYTB short fragment	CCTCCCATTATTATCGCCGCCCTTGC	GTCTGGGTCTCCTAGTAGGTCTGGGAAA
CYTB long fragment	AAAATCCCCGCAAACAATGACCACCC	GGCAATTAAGAGTGGGATGGAGCCAA

ANP, atrial natriuretic peptide; COL1A1, Collagen alpha-1 type I; TIMP1, tissue inhibitor matrix metalloproteinase 1; MCT1, monocarboxylate transporter 1; Bdh1, 3-hydroxybutyrate dehydrogenase 1; 36B4, acidic ribosomal protein 36B4.

Supplemental Table II. General characteristics in sham-operated and post-MI rats.

Parameters	Sham-Chow	Sham-KE-2	MI-Chow	MI-KE-2-E	MI-KE-2-L	P value
Caloric intake (kcal/day)	48.5 ± 3.5	45.5 ± 1.3	45.3 ± 2.8	44.6 ± 5.8	45.8 ± 3.3	0.119
Atria/TL (mg/mm)	1.32 ± 0.2	1.24 ± 0.1	1.79 ± 0.4 [†]	1.44 ± 0.2 [§]	1.50 ± 0.2 [§]	<0.001
Lungs/TL (mg/mm)	39.5 ± 2.3	38.8 ± 3.3	39.4 ± 3.0	38.4 ± 2.7	37.2 ± 2.4	0.244
Liver/TL (mg/mm)	326.2 ± 24.8	323.1 ± 17.1	314.7 ± 31.5	303.9 ± 31.5	313.6 ± 30.0	0.559
Left kidney/TL (mg/mm)	36.7 ± 3.5	35.4 ± 2.3	36.8 ± 3.6	37.3 ± 3.6	34.3 ± 3.8	0.214
Right kidney/TL (mg/mm)	35.4 ± 3.0	36.5 ± 1.5	37.9 ± 4.1	36.1 ± 2.2	36.3 ± 4.0	0.482
Spleen/TL (mg/mm)	18.2 ± 2.9	17.1 ± 1.8	17.7 ± 2.2	17.5 ± 2.5	17.9 ± 2.0	0.863
Plasma creatinine (μmol/l)	22 ± 2.7	22 ± 2.3	22.3 ± 2.6	23.2 ± 2.2	22.4 ± 2.3	0.87
Plasma sodium (mmol/l)	134.3 ± 1.3	134.7 ± 2.0	134.2 ± 0.9	134.7 ± 0.5	135.1 ± 1.6	0.65
Plasma potassium (mmol/l)	3.3 ± 0.2	3.5 ± 0.5	3.7 ± 0.4	3.7 ± 0.2	3.5 ± 0.3	0.201
Plasma insulin (ng/ml)	1.5 ± 0.6	0.9 ± 0.3 [*]	1.7 ± 1.0	1.1 ± 0.4	0.6 ± 0.4 [‡]	0.041
Plasma glucagon (pg/ml)	459.5 ± 134.2	406 ± 69.4	316.7 ± 49 [†]	314.9 ± 26.2 [#]	306.6 ± 42.5 [#]	<0.001

n=7-22. Data are presented as means ± SD. TL, tibia length.

*P<0.05 vs Sham-Chow

†P<0.01 vs Sham-Chow

‡P<0.05 vs MI-Chow

§P<0.01 vs MI-Chow

||P<0.05 vs. Sham-KE

#P<0.01 vs. Sham-KE

Supplemental references

15. Horton JL, Davidson MT, Kurishima C, Vega RB, Powers JC, Matsuura TR, Petucci C, Lewandowski ED, Crawford PA, Muoio DM, Recchia FA, Kelly DP. The failing heart utilizes 3-hydroxybutyrate as a metabolic stress defense. *JCI Insight*. 2019;4(4):e124079. doi: 10.1172/jci.insight.124079.
27. Weinheimer CJ, Lai L, Kelly DP, Kovacs A. Novel mouse model of left ventricular pressure overload and infarction causing predictable ventricular remodelling and progression to heart failure. *Clin Exp Pharmacol Physiol*. 2015;42:33–40.
28. Yurista SR, Silljé HHW, Oberdorf-Maass SU, Schouten E, Pavez Giani MG, Hillebrands J, van Goor H, van Veldhuisen DJ, de Boer RA, Westenbrink BD. Sodium-glucose co-transporter 2 inhibition with empagliflozin improves cardiac function in non-diabetic rats with left ventricular dysfunction after myocardial infarction. *Eur J Heart Fail*. 2019;21:862–873.
29. Yurista SR, Silljé HHW, Nijholt KT, Dokter MM, van Veldhuisen DJ, de Boer RA, Westenbrink BD. Factor Xa Inhibition with Apixaban Does Not Influence Cardiac Remodelling in Rats with Heart Failure After Myocardial Infarction. *Cardiovasc drugs Ther*. 2020. doi: 10.1007/s10557-020-06999-7.
30. Yurista SR, Silljé HHW, van Goor H, Hillebrands J-L, Heerspink HJL, de Menezes Montenegro L, Oberdorf-Maass SU, de Boer RA, Westenbrink BD. Effects of Sodium–Glucose Co-transporter 2 Inhibition with Empagliflozin on Renal Structure and Function in Non-diabetic Rats with Left Ventricular Dysfunction After Myocardial Infarction. *Cardiovasc Drugs Ther*. 2020;34:311–321.